ChemComm

# Towards Resolving the Spatial Metabolome with Unambiguous Molecular Annotations in Complex Biological Systems by Coupling Mass Spectrometry Imaging with Structures for Lossless Ion Manipulations



| | |
|---|---|
| Journal: | *ChemComm* |
| Manuscript ID | CC-COM-09-2018-007482.R1 |
| Article Type: | Communication |
| | |

ChemComm

COMMUNICATION

# Towards Resolving the Spatial Metabolome with Unambiguous Molecular Annotations in Complex Biological Systems by Coupling Mass Spectrometry Imaging with Structures for Lossless Ion Manipulations

Received 00th January 20xx,
Accepted 00th January 20xx

DOI: 10.1039/x0xx00000x

www.rsc.org/

Gabe Nagy [#a], Dusan Veličković [#a], Rosalie K. Chu [b], Alyssa A. Carrell [c], David J. Weston [c], Yehia M. Ibrahim [a], Christopher R. Anderton [*b], Richard D. Smith [*a]

**We demonstrate the coupling of liquid extraction surface analysis (LESA) to structures for lossless ion manipulations in conjunction with serpentine ultralong path with extending routing (SLIM SUPER) ion mobility-mass spectrometry (IM-MS) for the unambiguous annotation of important isomeric glycoforms in carbon-fixing communities.**

Mass spectrometry imaging (MSI) has increasingly become a part of the analytical toolbox, providing spatial distributions of the biomolecules within samples [1]. A variety of MSI capabilities and methods that have been reported, showing promise in elucidating cellular processes (e.g. as a function of resource availability, defense, and disease states). Currently, state of the art approaches for untargeted spatial metabolomics couple e.g. matrix-assisted laser desorption/ionization (MALDI) to ultra-high resolution MS, and are often capable of providing exact molecular formulas of analytes involved in localized biochemical processes [2]. A major bottleneck of current mass spectrometry imaging (MSI) methods is their inability to accurately and confidently delineate amongst isomers within a single probing area; single stage MS cannot distinguish isomers, and hence cannot provide confident annotation of molecular structures for imaged ions [3]. This can be problematic as structural and/or stereo-isomers may e.g. show substantially different physiological effects [4], create different surface epitopes [5], and portray different behaviors based on pathological or non-pathological conditions [6]. Use of tandem MS imaging ($MS^2I$) in a MALDI-MSI workflow can substantially improve molecular annotation, yet such efforts remain limited due to the ability to target a limited number of ions, as well as the substantially lower sensitivity or greater sample sizes required for larger numbers of targeted species [7]. Recently, Ellis et al. [8] described a novel automated MALDI-MSI method with data-dependent $MS^2$ acquisition of lipid species, where parallel full-scan FTMS and one IT-MS/MS (collision-induced dissociation in an ion trap) scan at an adjacent 20 µm position was accomplished, resulting in mapping and identification of lipids with 40 µm lateral resolution. However, this approach still leaves uncertainty that an ion species mapped in one tissue portion is identical to another in the tissue portion where the $MS^2$ spectrum was acquired. This problem is increasingly exacerbated for MSI of more complex and multi-organism systems [9]. Therefore, there is a need to develop approaches where MS/MS, or other orthogonal, analyses can be used to distinguish potentially ambiguous species imaged from the same sample area [10].

Liquid extraction surface analysis (LESA) is an imaging technique that benefits in having desorption and ionization steps decoupled, providing a constant flow of analytes to the MS analyzer over an extended period of time, and facilitating orthogonal analyses of numerous ions in a probed location [11]. Recently, Veličković et al. exploited this to perform tandem MS of numerous isobaric/isomeric analytes differently distributed over a complex microbiome sample, permitting increased confidence for molecular identification at each probed location [12]. However, it was observed that several isomeric disaccharide species were indistinguishable based on their fragmentation patterns alone [12], demonstrating the need for augmenting the MSI workflow for characterizing the spatial distributions of isomeric species.

Recently, the coupling of ion mobility (IM) to MSI has attracted attention for providing a pre-MS analysis separation step for ions in the gas-phase based on their shape dependent ion mobility [13]. This incorporation of IM into the MSI workflow has shown promise for the separation of analytes of interest from other isobaric species (e.g. lipids versus peptides) as well as from background/matrix interferences and chemical noise,

[a] Biological Sciences Division, Pacific Northwest National Laboratory, Richland, WA 99352
[b] Environmental Molecular Sciences Laboratory, Pacific Northwest National Laboratory, Richland, WA 99352
[c] Biosciences Division, Oak Ridge National Laboratory, Oak Ridge, TN 37830
# Authors contributed equally
* Emails: rds@pnnl.gov and christopher.anderton@pnnl.gov
Electronic Supplementary Information (ESI) available: [experimental conditions and individual IM peak assignments]. See DOI: 10.1039/x0xx00000x

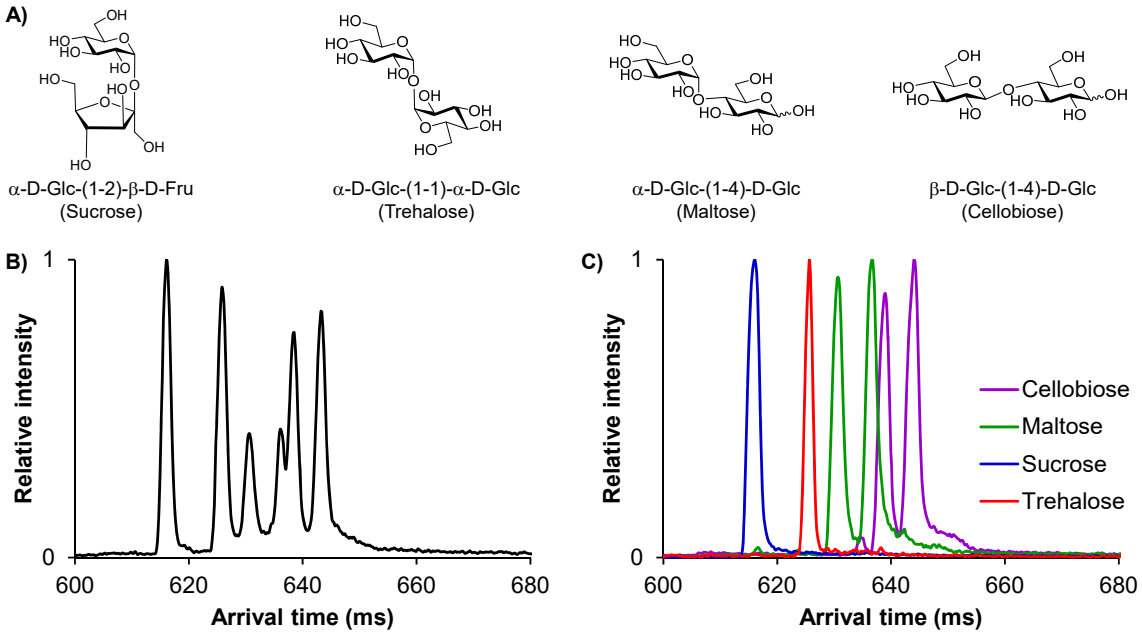


**Figure 1**. The four isomeric disaccharides hypothesized to be present in the tripartite sample (A). The 85.5 m SLIM SUPER IM separation of an isomeric mixture of the standards (B) and as the individual standards run separately (C). Ions were accumulated for 1 second 'in-SLIM' and separated as their [M+Na]+ adducts, 365.1 m/z.

to more accurately and confidently identify and characterize localized changes. Additionally, depending on the implementation, it can optimize ion utilization efficiency, increasing the numbers of species both detected and identified in MSI [3,13]. While promising, reported IM-MSI methods remain limited by the sensitivity of measurements (due substantially to their ion utilization efficiency) and more importantly, the IM separation power, or resolution [13] for distinguishing biologically-relevant isomers [14].

Recently, IM in structures for lossless ion manipulations (SLIM) utilizing serpentine ultralong path with extended routing (SUPER) has been developed to overcome the drawbacks of IM-MS platforms [15]. Specifically, SLIM SUPER IM separations benefit from high ion utilization efficiencies in conjunction with greatly extended separation path lengths providing large increases in both IM separation power and resolution [15]. Additionally, gains in sensitivity in SLIM are afforded by ion introduction and accumulation in the SLIM module itself, providing a two to three order of magnitude increase in number of ions utilized in each IM separation due to the much greater ion population sizes feasible [15]. (See Supporting Information for a comparison of signal intensities with both ion introduction methods).

Herein, we report the coupling of LESA with SLIM SUPER IM-MS for MSI of disaccharide isomers in a peatland model system composed of a co-culture of peat moss (*Sphagnum fallax*), cyanobacteria (*Nostoc muscorum*), and fungi (*Trizodia spp.*) cultivated on a solid agar medium, as previously described [12]. LESA-$MS^2$ imaging [12] previously revealed that non-reducing α-anomeric disaccharides were prevalent in both the fungus and moss regions, while reducing disaccharides were only visualized in the cyanobacteria region. Unfortunately, the disaccharides species were too similar in their $MS^2$ fragmentation patterns for unambiguous identification. The isomeric disaccharides most likely present are sucrose, trehalose, maltose, and cellobiose since sucrose is synthesized in oxygenic photosynthetic organisms [16], trehalose is an energy source that accumulates in high levels in both bacteria and fungi [17], and maltose and cellobiose can arise from glycogen and cellulose degradation (glycogen is the carbohydrate storage polysaccharide in thylakoids of cyanobacteria [18] and cellulose is a constituent of moss cell walls [19], respectively).

Initially, we developed a SLIM SUPER IM separation to resolve and characterize the disaccharide isomers (Figure 1A) whose structures only differ in their linkage positioning, α/β anomericity, and monosaccharide constituency (i.e., sucrose contains a fructose moiety, whereas all others are exclusively glucose-glucose disaccharides). Previous examples of IM separations of similar challenging disaccharide isomers were unable to resolve isomeric mixtures sufficiently to enable confident molecular identifications [20]. As shown in Figure 1B, we observed that all four disaccharides could be well resolved from one another after 85.5 meters of SLIM SUPER IM separation as their singly sodiated adducts; individual assignments are shown in Figure 1C. For more information on the SLIM SUPER IM-MS platform and experimental conditions used in these experiments, see the Supporting Information and elsewhere [15]. In this work the non-reducing sugars (sucrose and trehalose) both display single well resolved IM peaks, which we attribute to their inability to mutarotate into their individual α/β anomers, while the reducing maltose and cellobiose both exhibited two distinct mobility features hypothesized to be from their distinct α and β anomers. Furthermore, non-reducing

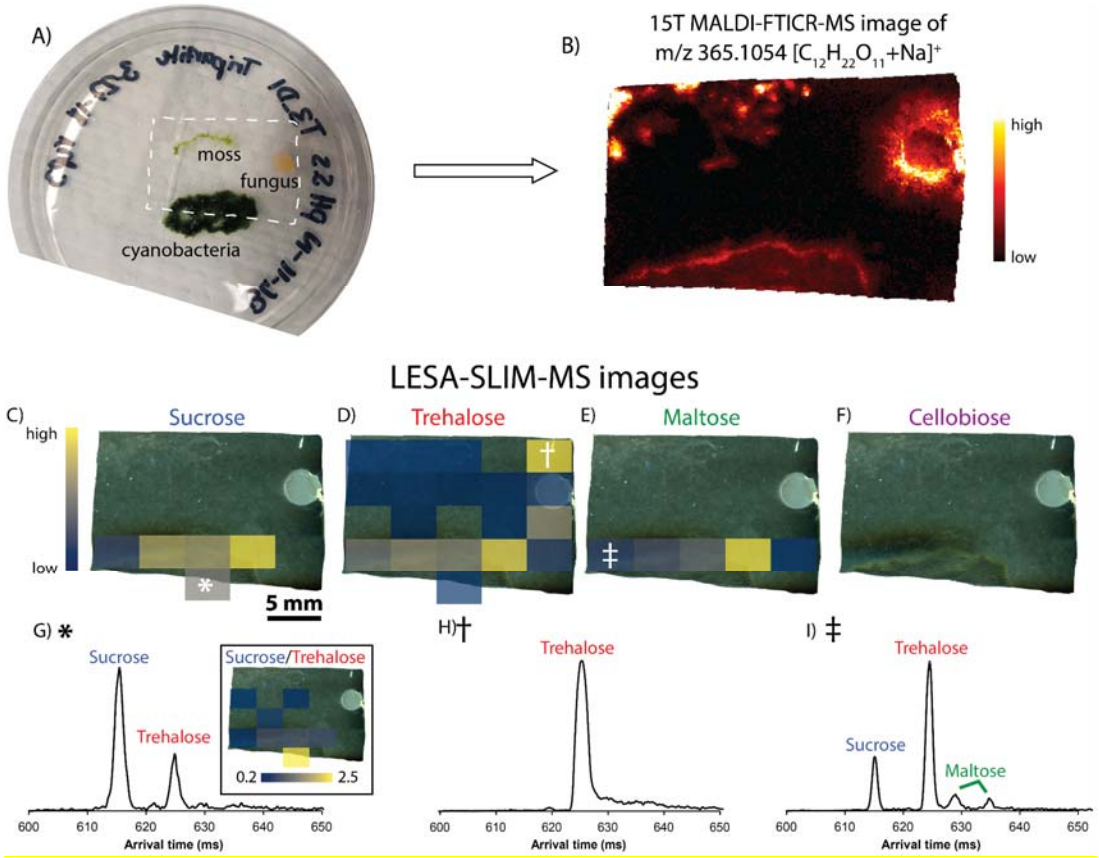


**Figure 2**. The tripartite culture of peat moss, cyanobacteria, and fungi grown on agar (A) was excised and studied using 15 Tesla MALDI FTICR-MS imaging, which providing an overall map of the disaccharide distribution with 200 µm pixel size (B). Post-MALDI-MSI with the LESA SLIM SUPER IM-MS imaging, at 3 mm spatial resolution, reveals the individual disaccharide distributions across the sample for sucrose (C), trehalose (D), maltose (E), and cellobiose (F). Different disaccharides profile over tripartite interaction zones are visualized through IM traces at m/z 365.1 in selected pixels *, †, and ‡ (G-I, respectively) with insert in (G) that shows the spatial relative abundance ratios of sucrose versus trehalose from *. IM traces of all 21 pixels, are provided in the Supporting Information.

disaccharides (sucrose and trehalose) both had higher mobilities, and thus more compact structures, than their non-reducing counterparts (maltose and cellobiose).

With these results demonstrating these isomeric glycoforms could be rapidly (<1 s) IM separated, we set out to assess the localized disaccharide profiles in our tripartite sample using LESA-SLIM SUPER IM-MSI. Figure 2 illustrates the LESA-SLIM SUPER IM-MSI workflow and output images created, as well as the MALDI MS-images of the tripartite sample taken before said analysis. The highly reproducible and resolvable separations for these isomeric disaccharides greatly increases the confidence in their identifications. While MALDI provides high spatial information about the overall disaccharide pool distribution, LESA-SLIM SUPER IM-MSI reveals their isomeric composition and yield over individual tripartite constituents and interaction zones. Each LESA-SLIM SUPER IM-MSI image displays the extracted MS signal intensity of each disaccharide at a given location (i.e. pixel) as determined by their arrival times/mobility peaks. For maltose and cellobiose, we used the sum of both mobility peaks to create their respective images. (See Supporting Information for the IM separations for each pixel).

From Figure 2, it was observed that the disaccharide profile varied from pixel-to-pixel, indicating variations in disaccharide accumulation in the tripartite constituents. While sucrose and maltose are evident only in the cyanobacteria colony, trehalose was observed for each member of the tripartite community. Interestingly, inside the cyanobacteria colony, the sucrose concentration gradually increases toward the interaction zone with the fungus (Figure 2D), which may imply enhanced nitrogen fixation activity through carbon flux in this area [16]. On the edges of the cyanobacteria colony, the sucrose amounts are ~5-fold less abundant compared to that of trehalose (Figure 2H, insert), but remains the dominant disaccharide within the colony. This may indicate that bacterial cells in the outer areas of the colony have had more exposure to environmental stress, and thus triggered an increased synthesis of trehalose to serve as a protectant from desiccation, dehydration, heat, cold, and oxidation [17]. We detected a third isomer, maltose, to be present in the disaccharide pool in some areas of cyanobacteria colony, which perhaps arises from enzymatic and/or non-specific hydrolysis of glycogen-like granules that were previously described in this very same bacterial species [18]. We found trehalose as the only disaccharide in moss, which corresponds to previous findings noting this sugar serves as a signaling

molecule in plants [17]. Notably, no cellobiose was observed in any of the imaged pixels, indicating no biological cellulose degradation occurred, at least not via this intermediate.

These results validate the previously established LESA-MS/MS approach [12] and speculation that reducing sugars (now revealed to be maltose and not cellobiose) are the most dominant in cyanobacteria, while fungus is the richest in non-reducing α-anomeric sugars (now revealed to be trehalose and not sucrose). Here, we additionally achieved insights into the changing glycoprofile within this tripartite interaction due to the high-resolution IM separation capabilities provided by the SLIM platform. The SLIM SUPER extended 85.5 m path IM permitted fully resolving isomeric disaccharides that could not be distinguished in previous $MS^2$ measurements. These results provide new insights into the glyco-composition in this carbon-fixing community. Moreover, SLIM SUPER IM was able to resolve these isomeric disaccharides with increased sensitivity in a fast/high-throughput fashion (<1 s), providing increased confidence in the identification and location of important isomeric carbohydrates in MSI through the coupling with LESA. We envision this methodology will be broadly applicable to other mass spectrometry imaging modalities and invaluable in multiplexed, untargeted, analyses of a single probing location.

Experiments were performed at EMSL, sponsored by the Office of Biological and Environmental Research (BER), U.S. Department of Energy (DOE). EMSL is located at PNNL, a multidisciplinary national laboratory operated by Battelle for the U.S. DOE under contract DE-AC05-76RL0 1830 for the DOE. This work was partially supported by the National Institute of General Medical Sciences (P41 GM103493).

## Conflicts of interest

There are no conflicts to declare.

## Notes and references

1 R. M. Caprioli, *PROTEOMICS* 2016, **16**, 1607.
2 A. Palmer, D. Trede, T. Alexandrov, *Metabolomics* **2016**, 12, 107.
3 S. A. Stopka, B. J. Agtuca, D. W. Koppenaal, L. Pasa-Tolic, G. Stacey, A. Vertes, C. R. Anderton, *Plant J.* **2017**, 91, 340.
4 D. Veličković, N. Milosavić, Bezbradica, Dejan, F. Bihelović, A. M. Segal, D. Šegan, J. Trbojević, A. Dimitrijević, *Appl. Microbiol. Biotechnol*. **2014**, 98, 6317; I. Churruca, A. Fernandez-Quintela, M. P. Portillo, *BioFactors* **2009**, 35, 105.
5 K. Takahashi, A. D. Smith, K. Poulsen, M. Kilian, B. A. Julian, J. Mestecky, J. Novak, M. B. Renfrow, *J. Proteome Res*. **2012**, 11, 692.
6 J. M. Prien, L. C. Huysentruyt, D. J. Ashline, A. J. Lapadula, T. N. Seyfried, V. N. Reinhold, *Glycobiology* **2008**, 18, 353.
7 D. C. Perdian, Y. J. Lee, *Anal. Chem*. **2010**, 82, 9393; K. A. Lunsford, G. F. Peter, R. A. Yost, *Anal. Chem*. **2011**, 83, 6722.
8 S. R. Ellis, M. R. L. Paine, G. B. Eijkel, J. K. Pauling, P. Husen, M. W. Jervelund, M. Hermansson, C. S. Ejsing, R. M. A. Heeren, *Nature Methods* **2018**, 15, 515.
9 D. Veličković, B. J. Agtuca, S. A. Stopka, A. Vertes, D. W. Koppenaal, L. Paša-Tolić, G. Stacey, C. R. Anderton, *The ISME Journal* **2018**, 12, 2335.
10 R. L. Hansen, Y. J. Lee, *J. Am. Soc. Mass Spectrom*. **2017**, 28, 1910-1918.; D. Veličković, C. R. Anderton, *Rhizosphere* **2017**, 3, 254.
11 D. Eikel, M. Vavrek, S. Smith, C. Bason, S. Yeh, W. A. Korfmacher, J. D. Henion, *Rapid Commun. Mass Spectrom*. **2011**, 25, 3587.
12 D. Veličković, R. K. Chu, A. A. Carrell, M. Thomas, L. Pasa-Tolic, D. J. Weston, C. R. Anderton, *Anal. Chem*. **2018**, 90, 702.
13 M. Sans, C. L. Feider, L. S. Eberlin, Curr. Opin. Chem. Biol. 2018, 42, 138; M. Winter, A. Tholey, A. Kristen, C. Rocken, *PROTEOMICS* **2017**, 17, 1700236; J. A. McLean, W. B. Ridenour, R. M. Caprioli, *J. Mass Spectrom*. **2007**, 42, 1099; M. C. Laura, K. Mahmoud, S. Haywood-Small, M. T. Gillian, D. P. Smith, M. R. Clench, *Rapid Commun. Mass Spectrom*. **2013**, 27, 2355; C. L. Feider, N. Elizondo, L. S. Eberlin, Anal. Chem. 2016, 88, 11533; R. L. Griffiths, A. J. Creese, A. M. Race, J. Bunch, H. J. Cooper, *Anal. Chem*. **2016**, 88, 6758.
14 C. Manz, K. Pagel, *Curr. Opin. Chem. Biol*. **2018**, 42, 16; J. Hofmann, K. Pagel, *Angew. Chem. Int. Ed*. **2017**, 56, 8342; J. Hofmann, H. S. Hahm, P. H. Seeberger, K. Pagel, *Nature* **2015**, 526, 241.
15 L. Deng, S. V. B. Garimella, A. M. Hamid, I. K. Webb, I. K. Attah, R. V. Norheim, S. A. Prost, X. Zheng, J. A. Sandoval, E. S. Baker, Y. M. Ibrahim, R. D. Smith, *Anal. Chem*. **2017**, 89, 6432; L. Deng, Y. M. Ibrahim, E. S. Baker, N. A. Aly, A. M. Hamid, X. Xhang, X. Zheng, S. V. B. Garimella, I. K. Webb, S. A. Prost, J. A. Sandoval, R. V. Norheim, G. A. Anderson, A. V. Tolmachev, R. D. Smith, *ChemistrySelect* **2016**, 1, 2396; L. Deng, I. K. Webb, S. V. B. Garimella, A. M. Hamid, X. Zheng, R. V. Norheim, S. A. Prost, G. A. Anderson, J. A. Sandoval, E. S. Baker, Y. M. Ibrahim, R. D. Smith, *Anal. Chem*. **2017**, 89, 4628; S. V. Garimella, A. M. Hamid, L. Deng, Y. M. Ibrahim, I. K. Webb, E. S. Baker, S. A. Prost, R. V. Norheim, G. A. Anderson, R. D. Smith, *Anal. Chem*. **2016**, 88, 11877; L. Deng, Y. M. Ibrahim, A. M. Hamid, S. V. Garimella, I. K. Webb, X. Zheng, S. A. Prost, J. A. Sandoval, R. V. Norheim, G. A. Anderson, A. V. Tolmachev, E. S. Baker, R. D. Smith, *Anal. Chem*. **2016**, 88, 8957; C. D. Chouinard, G. Nagy, I. K. Webb, T. Shi, E. S. Baker, S. A. Prost, T. Liu, Y. M. Ibrahim, R. D. Smith, *Anal. Chem*. 2018, DOI: 10.1021/acs.analchem.8b02397.
16 A. M. a. Kolman, N. C. Nishi, M. Perez-Cenci, L. G. Salerno, *Life* **2015**, 5.
17 A. D. Elbein, Y. T. Pan, I. Pastuszak, D. Carroll, *Glycobiology* **2003**, 13, 17.
18 L. Chao, C. C. Bowen, *J. Bacteriol*. **1971**, 105, 331.
19 A. Roberts, E. Roberts, C. Haigler, *Front. Recent Dev. Plant Sci*. **2012**, 3, 166.
20 S. Lee, S. J. Valentine, J. P. Reilly, D. E. Clemmer, *Int. J. Mass Spectrom*. **2012**, 309, 161; H. Li, B. Bendiak, F. Siems William, R. Gang David, H. Hill Herbert, *Rapid Commun. Mass Spectrom.* **2013**, 27, 2699; W. Gabryelski, K. L. Froese, *J. Am. Soc. Mass Spectrom*. **2003**, 14, 265; M. r. Fasciotti, B. Sanvido Gustavo, G. Santos Vanessa, M. Lalli Priscila, M. McCullagh, S. í. G. F, J. Daroda Romeu, G. Peter Martin, N. Eberlin Marcos, *J. Mass Spectrom*. **2012**, 47, 1643; B. H. Clowers, P. Dwivedi, W. E. Steiner, H. H. Hill, B. Bendiak, *J. Am. Soc. Mass Spectrom*. **2005**, 16, 660; Y. Huang, E. D. Dodds, *Anal. Chem*. **2013**, 85, 9728; P. Dwivedi, B. Bendiak, B. H. Clowers, H. H. Hill, *J. Am. Soc. Mass Spectrom*. **2007**, 18, 1163; X. Zheng, X. Zhang, N. S. Schocker, R. S. Renslow, D. J. Orton, J. Khamsi, R. A. Ashmus, I. C. Almeida, K. Tang, C. E. Costello, R. D. Smith, K. Michael and E. S. Baker, *Anal. Bioanal. Chem.*, 2017, **409**, 467.

 

**TOC Graphic:**